Supplementary Information

Supplementary Figures and Figure Legends

Supplementary Figure 1

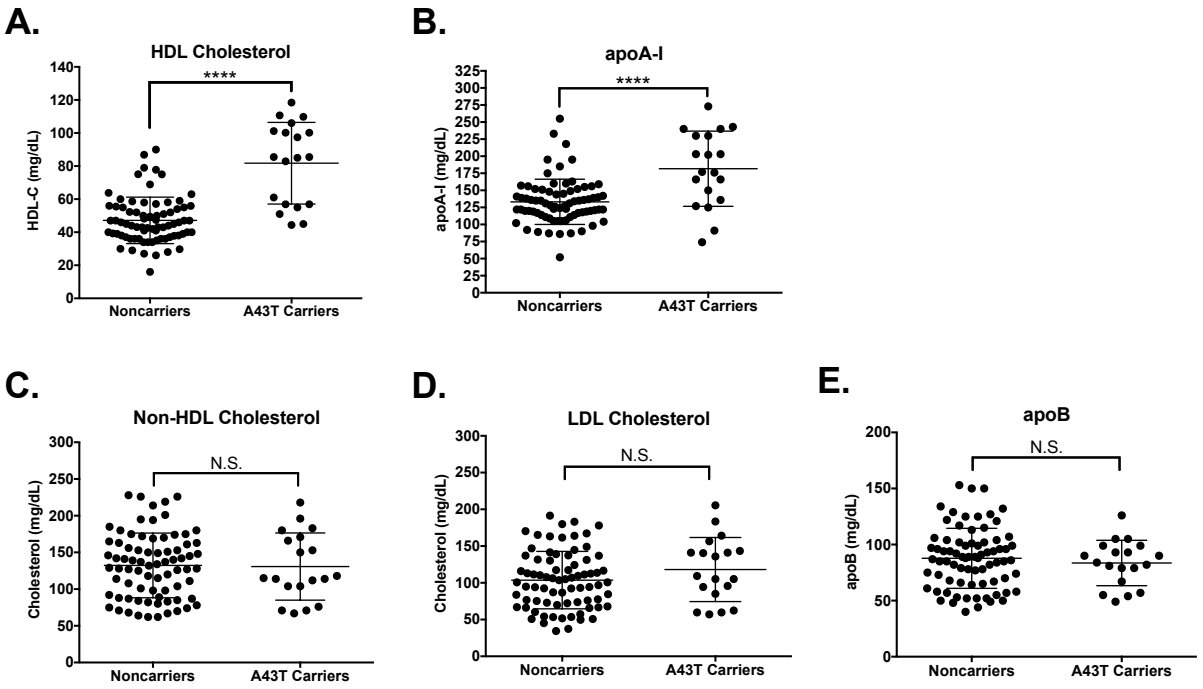

Supplementary Figure 1: Lipid and apolipoprotein measurements in carriers of the *APOC3* A43T variant vs. noncarrier controls in the Penn Medicine BioBank and HHDL cohorts. A. HDL-C in overnight fasted plasma of all identified A43T carriers and age- and gender-matched noncarriers. **B.** ApoA-I concentrations in the plasma samples from A. **C.** Non-HDL cholesterol in overnight fasted plasma of A43T carriers vs. noncarriers from A. **D.** LDL-C concentrations from plasma samples in A**. E.** ApoB concentrations in A43T variant carriers vs. controls from plasma samples in A. All measurements show data with N=19 A43T carriers and N=21 matched noncarriers. For all data, mean ± S.D. where appropriate, and data points show biological replicates. ****P<0.0001, Student's unpaired two-tailed T-test.

Supplementary Figure 2

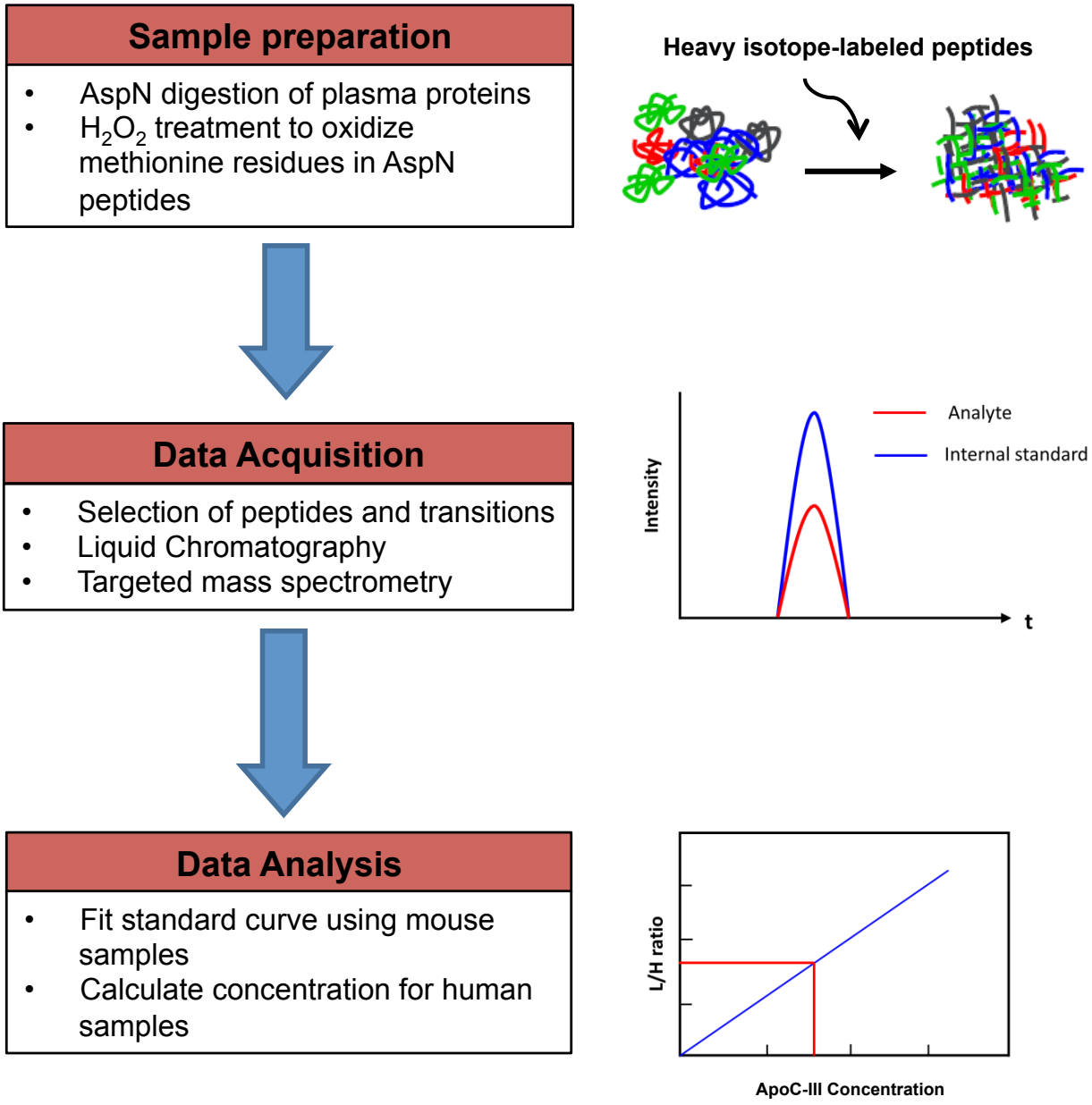

Supplementary Figure 2: Schematic illustration of the targeted mass spectrometry assay workflow. Approach for development and implementation of human-specific WT vs. A43T apoC-III isoform targeted multiple reaction monitoring assays is shown.

Supplementary Figure 3

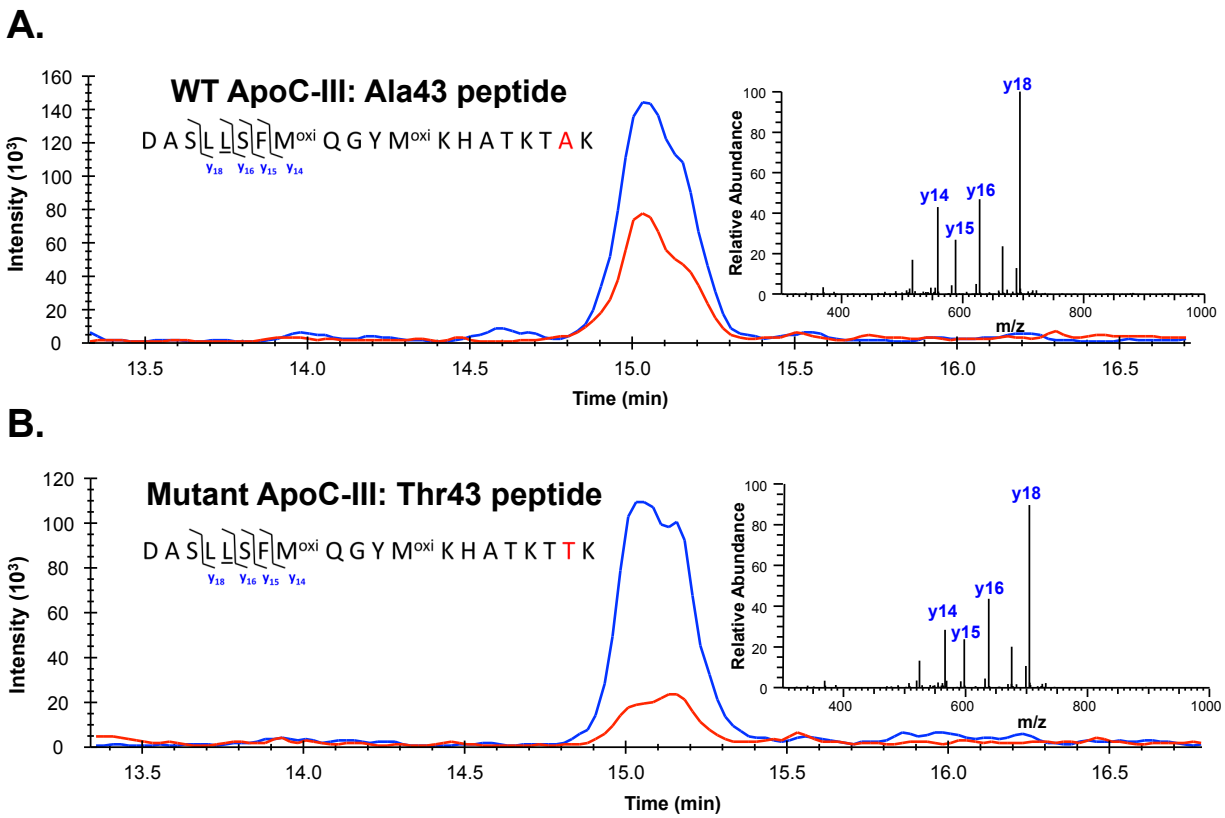

Supplementary Figure 3: Example LC-MS/MS data showing the extracted ion chromatograms for the native peptide (blue) and isotopically labeled peptide standards (red). The peptide sequence and product ion spectra for the AspN-generated 20 amino acid peptide corresponding to WT (**A**) and mutant apoC-III (**B**) are included above each chromatogram. The position of the variant amino acid between WT and mutant peptides is highlighted in red.

Supplementary Figure 4

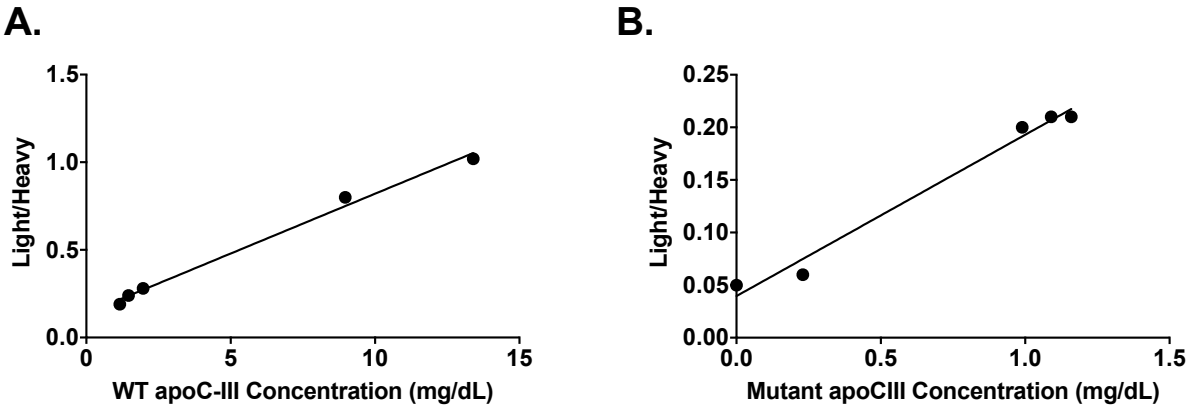

Supplementary Figure 4: external LC-MS/MS calibration curve. Five mouse plasma samples from mice expressing either human WT or A43T *APOC3* via AAV expression with known WT and A43T mutant apoC-III concentration were used as external calibrators to determine WT (**A**) and A43T mutant (**B**) apoC-III concentration in human samples. These samples were processed and analyzed in parallel with other human plasma samples. Linear regression was used to fit standard curves.

Supplementary Figure 5

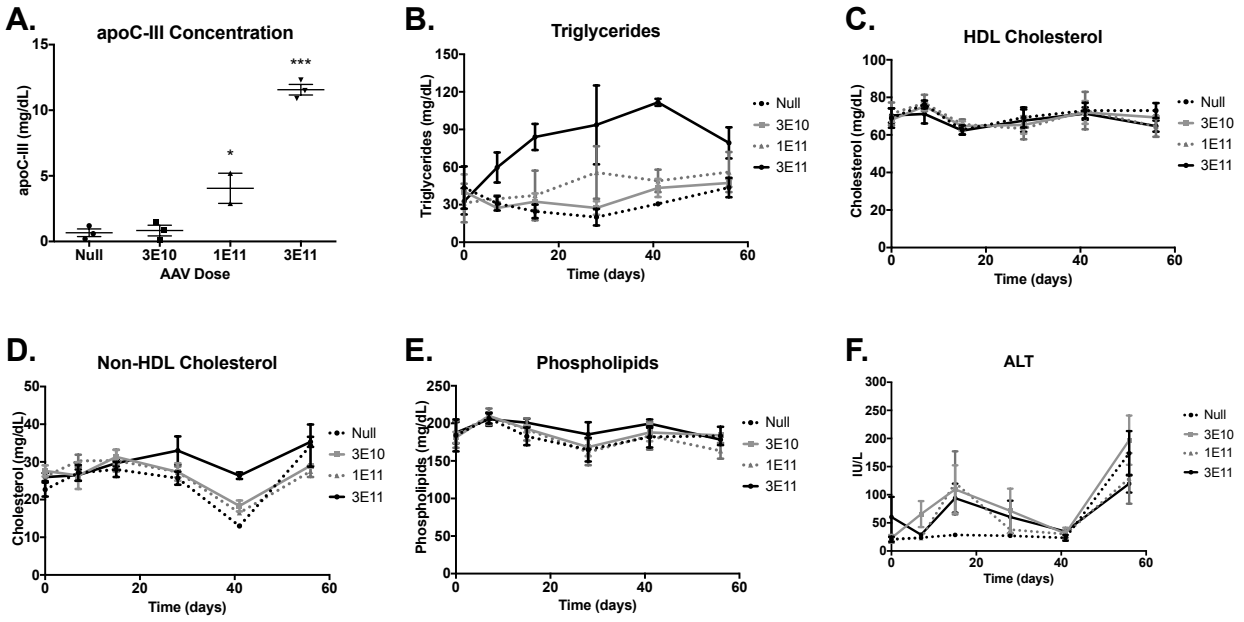

Supplementary Figure 5: Dose-optimization studies of WT *APOC3* AAV in mice. A. Plasma human ApoC-III concentration in C57BL/6 WT mice administered the indicated doses (genome copies of vector per mouse) of WT *APOC3* AAV by intraperitoneal injection (N=3 mice per group). Measurements were made eight weeks after AAV administration. **B.** Plasma TGs from four hour fasted plasma from mice in A over eight weeks. **C.** Plasma HDL-C from mice in A. **D.** Plasma Non-HDL-C in mice from A. **E.** Plasma phospholipids from mice in A. **F.** Plasma alanine aminotransferase (ALT) levels in mice from A. For all panels, N=3 mice per group. All data was replicated once by an independent repeat experiment. All measurements show mean ± S.E.M. where appropriate and data show biological replicates. *P<0.05, ***P<0.001, Student's unpaired two-tailed T-test compared to Null group.

Supplementary Figure 6

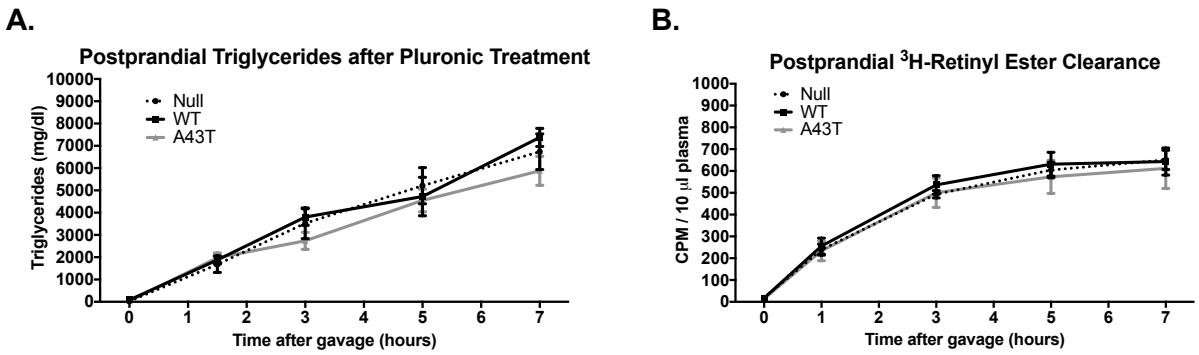

Supplementary Figure 6: Postprandial TG and chylomicron particle clearance in WT vs. A43T expressing mice. A. *Apoc3* KO mice expressing Null, *APOC3* WT or A43T AAVs and co-expressing CETP for four weeks were fasted overnight. They were then treated with Poloxamer P407 (Pluronic) in PBS (1 mg/kg fasting body weight) intravenously by tail-vein injection, and then immediately gavaged with olive oil (10 µl/g fasting body weight). Plasma was collected from mice at 0, 1.5, 3, 5, and 7 hours following Pluronic administration and gavage and used to measure TG levels. **B.** A separate cohort of mice in the same described groups as in **A** were fasted overnight and then subjected to gavage with ^{3}H-retinol (10 µCi) mixed with 250 µl of olive oil. Plasma ^{3}H activity was measured from 10 µl of plasma from each mouse as a measure of ^{3}H-retinyl ester levels, a marker of chylomicron particle number. ^{3}H-retinyl ester activity was measured through seven hours after gavage. For both panels, N=6 mice per group. All measurements show mean ± S.E.M. where appropriate and data show biological replicates.

Supplementary Figure 7

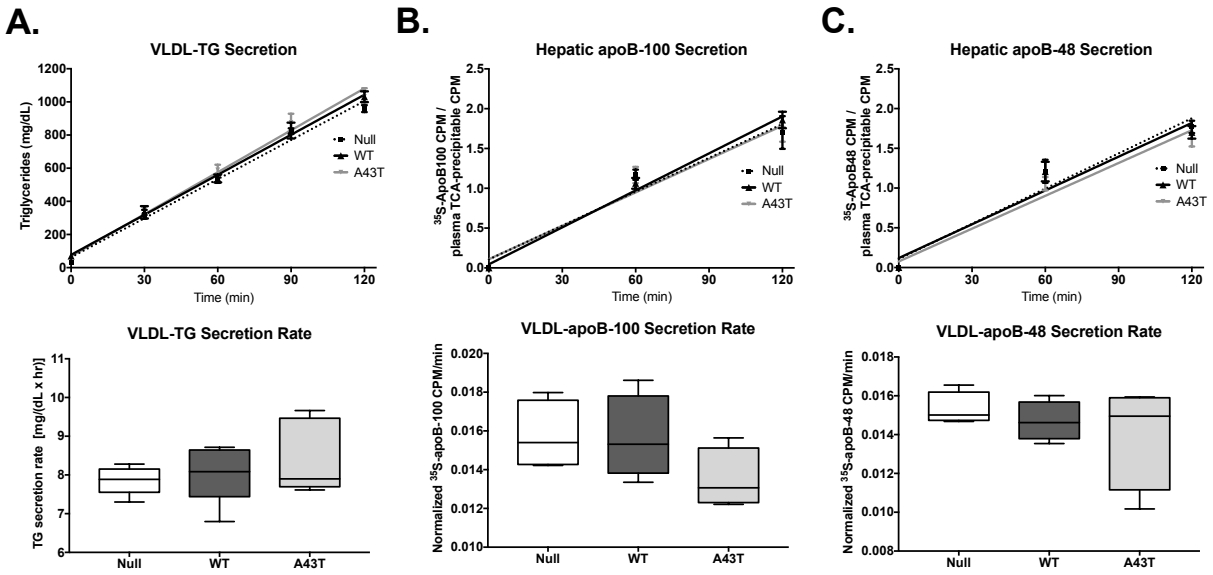

Supplementary Figure 7: VLDL TG and apoB secretion in mice expressing WT vs. A43T *APOC3*. A. (top) Plasma TG levels over time after Poloxamer P407 and ^{35}S administration in WT mice expressing Null or *APOC3* AAVs for four weeks. Curves were fitted to a line in GraphPad Prism. (bottom) Secretion rates as measure by the slope of the curves at the top. **B.** (top) Plasma ^{35}S-apoB-100 activity (normalized to activity in 2 µl of plasma after TCA precipitation) for mice expressing the indicated transgenes four weeks after AAV administration. ApoB-100 bands were excised from gels after SDS-PAGE and activity measured by scintillation counting and normalized to the TCA precipitable activity from plasma from the same plasma samples. (bottom) Secretion rates as measure by the slope of the curves at the top. **C.** Plasma ^{35}S-apoB-48 activity from mice in A and B. ApoB-48 bands were excised after SDS-PAGE, measured for activity and normalized to TCA precipitable activity from the same plasma samples. (bottom) Secretion rates as measured by the slope of the curves at the top. For all data,

N=6 mice per group, and data was replicated twice by two repeat experiments in independent cohorts of mice. For data in bottom sections of panels A-C, box length spans 25th to 75th percentile range of the data points, with the middle line indicating the median, and whiskers indicating the minimum and maximum values for the given data set. Data in top sections of panels A-C show mean ± S.E.M. where appropriate and data shows biological replicates.

Supplementary Figure 8

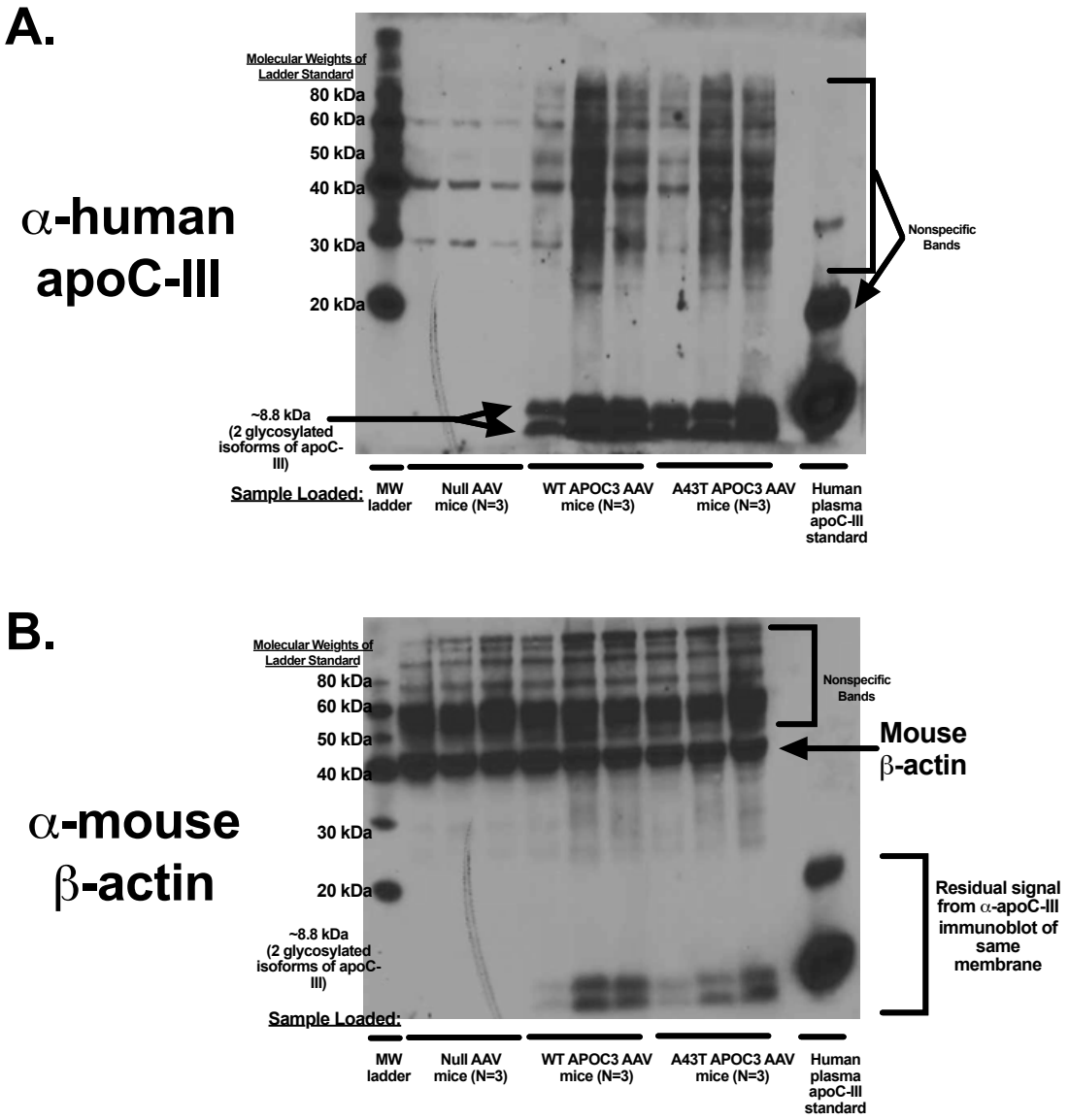

Supplementary Figure 8: Original images from immunoblots shown in Figure 2. Uncropped Hyblot CL films of the images in Figure 2M are shown. A. Uncropped film for anti-apoC-III immunoblot in Figure 2M. B. Uncropped film for anti-actin immunoblot in Figure 2M.

Supplementary Figure 9

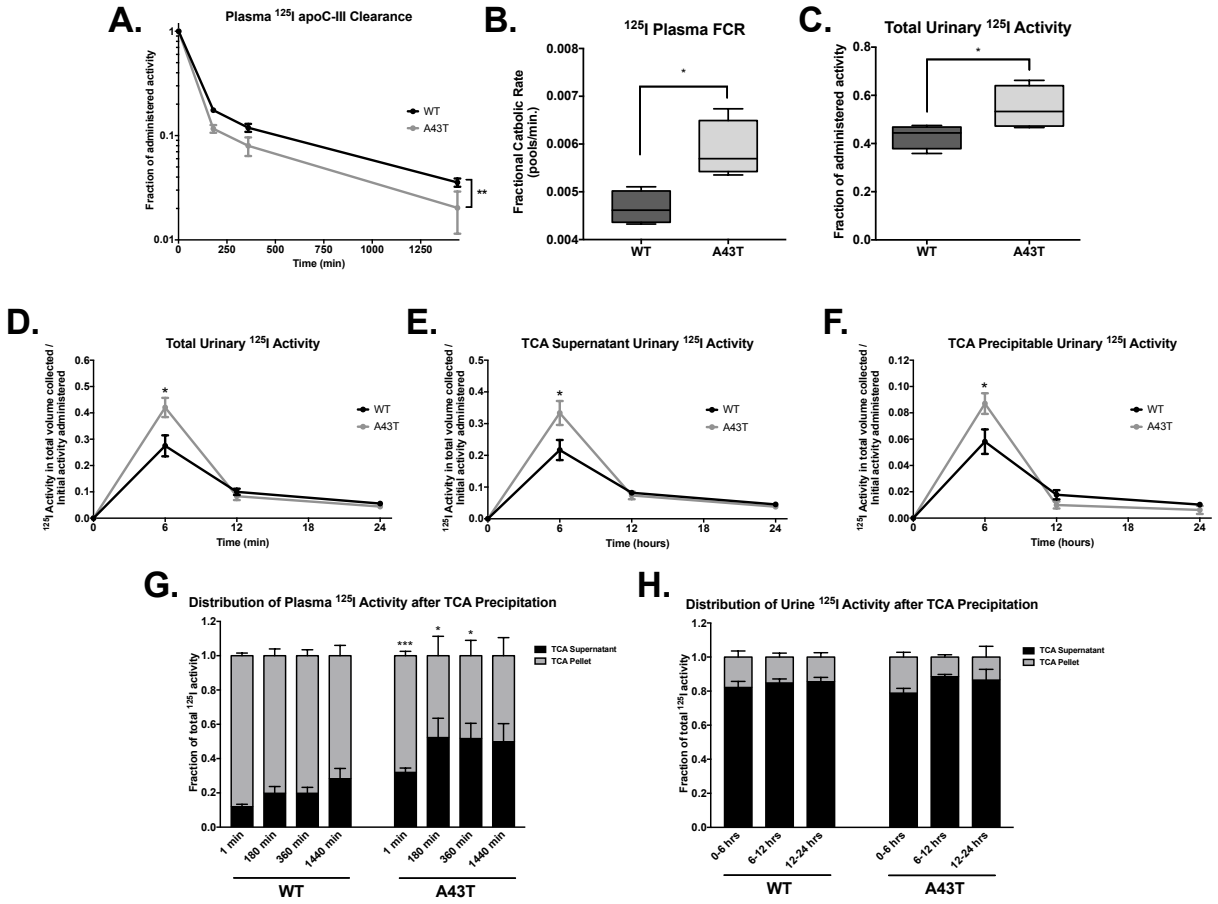

Supplementary Figure 9: Urinary clearance of ^{125}I-labeled WT vs. A43T apoC-III in mice. A. Plasma ^{125}I clearance curves over 24 hours for radiolabeled WT vs. A43T apoC-III in WT mice expressing either WT or A43T *APOC3* AAVs (N=4 mice per group). Mice expressing WT *APOC3* AAV received WT iodinated ApoC-III by intravenous administration and A43T *APOC3*-expressing mice received iodinated A43T apoC-III protein. **B.** Fractional catabolic rate of plasma ^{125}I activity, as measured by WinSAAM multi-exponential modeling program. Catabolic rates were calculated for each mouse individually. **C.** Total ^{125}I activity measured in urine collected from WT vs. A43T expressing mice at the end of 24 hours of collection following intravenous ^{125}I ApoC-III administration. **D.** Total urinary ^{125}I activity at the indicated time intervals over the

course of the ^{125}I apoC-III clearance study. Urine was collected individually at the indicated timepoints for each mouse and ^{125}I activity was measured and removed from metabolic cages prior to the next collection period up through 24 hours. **E.** ^{125}I activity in TCA soluble fraction of urine collected from each mouse at the indicated time intervals. 20 µl of urine was subjected to TCA precipitation and TCA soluble fractions were collected and re-measured for ^{125}I activity. The fraction of the 20 µl of urinary ^{125}I activity appearing in the TCA soluble fraction was used to calculate the proportion of TCA soluble ^{125}I activity in the total urine collected for each mouse for the indicated time intervals. **F.** ^{125}I activity in the TCA precipitable fraction of the urine collected from each mouse at the indicated time intervals from samples used in **D**. **G.** Fraction of plasma ^{125}I activity in TCA supernatant vs. pellet for each timepoint from 20 µl of plasma from mice administered ^{125}I-labeled WT vs. A43T apoC-III. Total plasma ^{125}I activity was measured for each mouse and subsequently TCA precipitation and measurement of activity in soluble vs. precipitable fractions was performed. **H.** Fraction of urinary ^{125}I activity in TCA supernatant vs. pellet for each time interval of urine collection for mice administered ^{125}I labeled WT vs. A43T apoC-III. TCA soluble vs. precipitable ^{125}I activity was measured from 20 µl of urine for each mouse for each time interval as indicated in **D-E**. For all panels, N=4 mice per group. For data in panels B-C, box length spans 25th to 75th percentile range of the data points, with the middle line indicating the median, and whiskers indicating the minimum and maximum values for the given data set. All other measurements show mean ± S.E.M. where appropriate, and all data shows biological replicates. For A, **P<0.01, two-way ANOVA of WT vs. A43T clearance curves. For B-F, *P<0.05, ***P<0.001, Student's unpaired T-test. For F, comparisons

are of the fraction of total activity in TCA precipitable fraction for WT vs. A43T for a given time interval.

Supplementary Figure 10

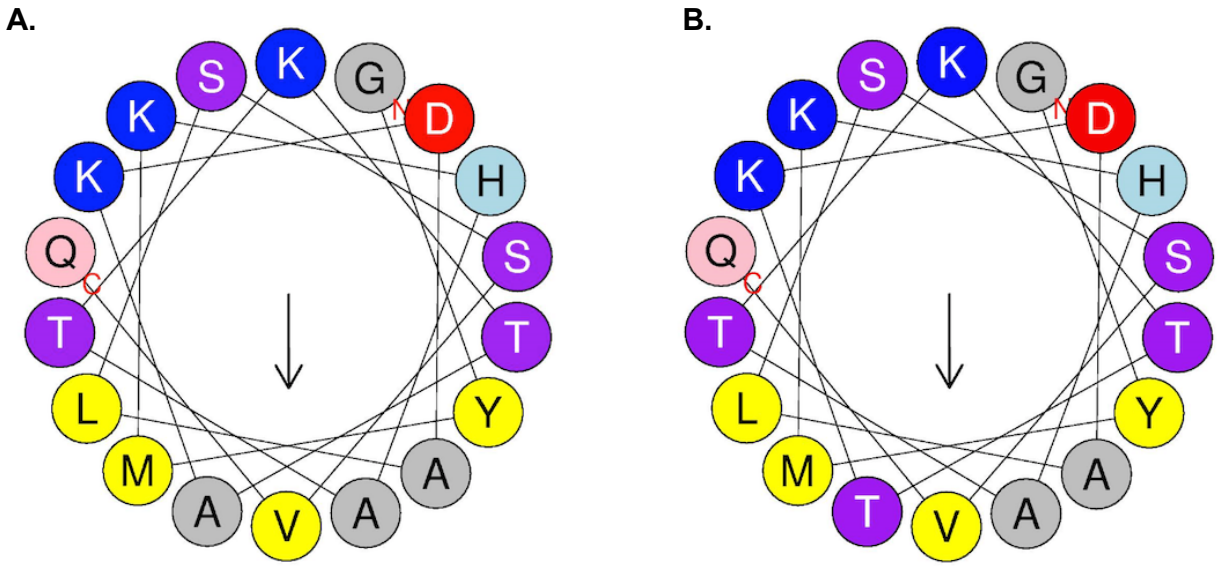

Supplementary Figure 10: Helical wheel diagrams of the 18-residue human apoC-III peptide 34-51 of the full-length apoC-III sequence (peptide 14-31 of the mature form which lacks the first 20 residues, which are the signal peptide). A. Helical wheel for the wild type peptide which contains A43 (A23 of the mature form) - the N-terminal residue G and C-terminal residue Q are marked. The vector of the helical hydrophobic moment is perpendicular (black arrow) with the hydrophobic face of the amphipathic α-helix, which contains the 7 amino acids LMAVAAY oriented towards the bottom of the picture (A43 is located between residues M and V). **B.** equivalent helical wheel for the A43T variant showing that the hydrophobic face is now LMTVAAY. The helical wheels were constructed using the program Heliquest (www. heliquest.ipmc.cnrs.fr).

Supplementary Figure 11

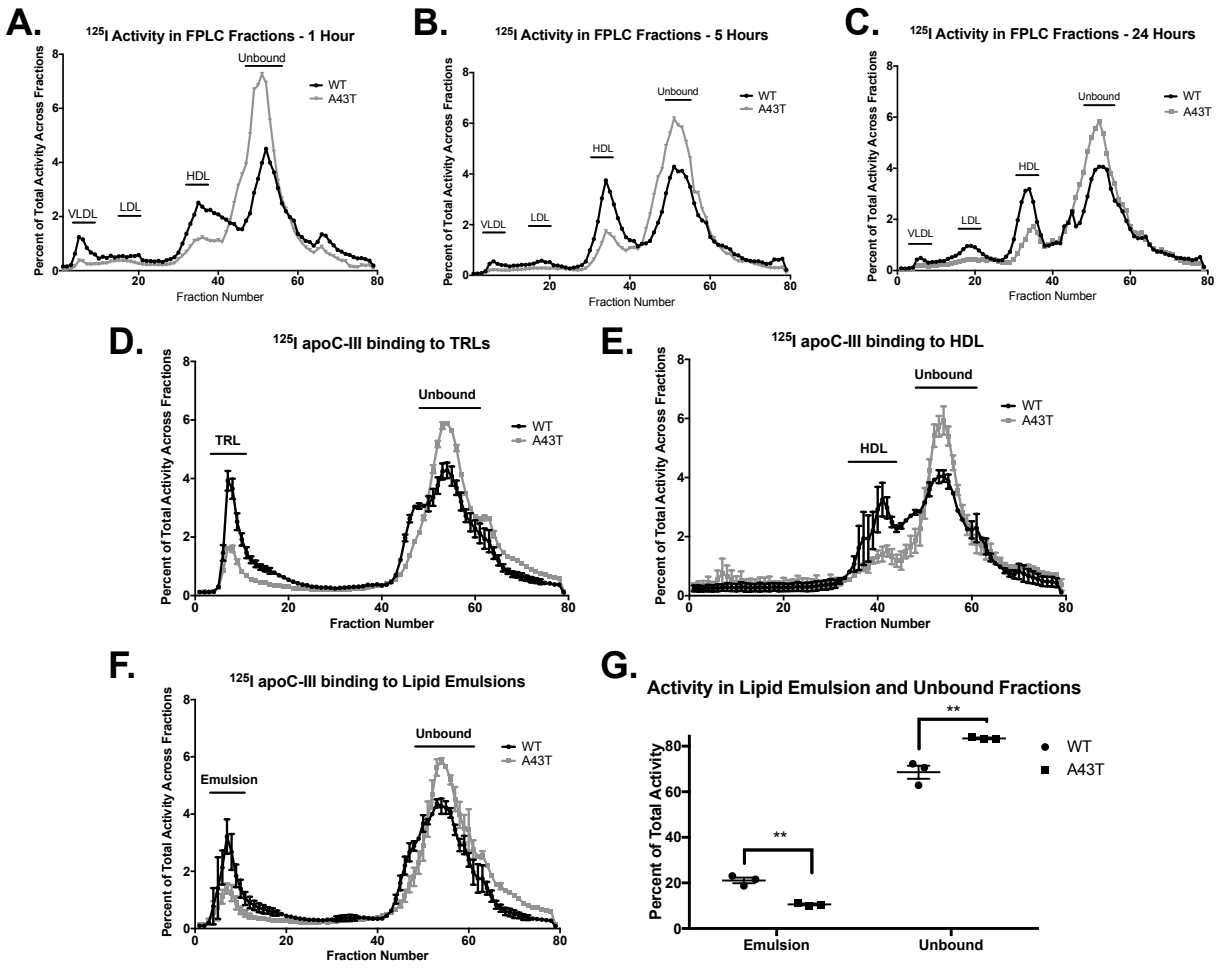

Supplementary Figure 11: Binding of WT vs. A43T apoC-III to lipid and human lipoprotein fractions. A. ^{125}I activity from FPLC-separated fractions of human plasma after incubation of ^{125}I-labeled WT vs. A43T apoC-III with human plasma (1 µg apoC-III and 200 µl plasma) for 1 hour at 37 °C. Activity is expressed as the fraction of total ^{125}I activity in the apoC-III:plasma mixture prior to FPLC separation. **B.** ^{125}I activity from FPLC-separated fractions of human plasma incubated with ^{125}I-labeled WT vs. A43T apoC-III for 5 hours at 37 °C. **C.** ^{125}I activity from FPLC-separated fractions from human plasma incubated with ^{125}I-labeled WT vs. A43T apoC-III for 24 hours at 37 °C. **D.** ^{125}I

activity from FPLC-separated fractions of human TRLs incubated with ^{125}I-labeled WT vs. A43T apoC-III (1 μg apoC-III and 100 μg TRL protein) for 1 hour at 37 °C. Graphs show mean ± S.D. of three replicate experiments. **E.** ^{125}I activity from FPLC-separated fractions of human HDL_3 incubated with ^{125}I-labeled WT vs. A43T apoC-III (1 μg apoC-III and 200 μg HDL_3 protein) for 1 hour at 37 °C. Graphs show ± S.D. of three replicate experiments. **F.** ^{125}I activity from FPLC-separated fractions of large lipid emulsions incubated with ^{125}I-labeled WT vs. A43T apoC-III for 1 hour at 37 °C. Graphs show ± S.E.M. of three replicate experiments. **G.** Relative ^{125}I activity in lipid emulsion fractions vs. unbound protein fractions from experiments in F. Bars indicate sum of relative amount of activity in fractions from three replicate experiments. All measurements show mean ± S.D. where appropriate and data shows biological replicate values. All data was replicated once by an independent repeat experiment. For A-C and G, **P<0.01, Student's unpaired two-tailed T-test.

Supplementary Figure 12

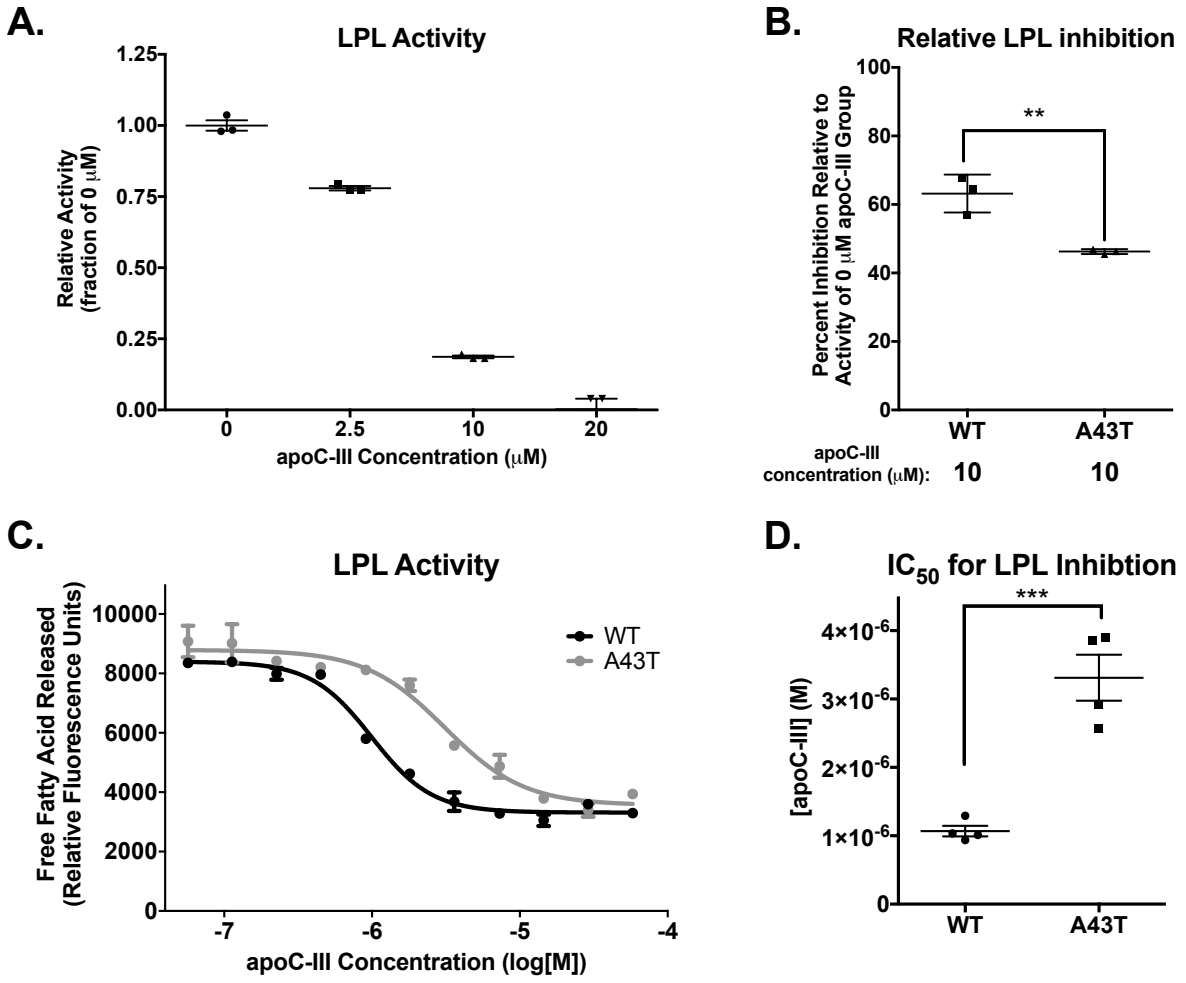

Supplementary Figure 12: Impact of A43T on LPL Inhibition by apoC-III. A. Relative LPL activity against ^{3}H-triolein labeled large lipid emulsion substrate with increasing reaction concentrations of WT apoC-III. LPL activity was measured as the amount of ^{3}H-oleic acid released over 30 minutes of incubation at 37 °C. Data is shown as the fraction of ^{3}H-oleic acid released relative to that from the 0 μM apoC-III group. Each bar represents triplicate reactions. **B.** Relative LPL inhibition of WT vs. A43T apoC-III using the assay in A comparing the two forms of apoC-III at equivalent reaction

concentrations. LPL inhibition is graphed as the relative difference in LPL activity between a 0 μM apoC-III group and each of the apoC-III groups (WT and A43T). 10 μM of WT or A43T apoC-III was used for these reactions. All reactions took place for 30 minutes at 37 °C and were performed in triplicate. **C.** Relative LPL activity against an Intralipid emulsion substrate with concentrations of WT or A43T apoC-III as indicated. LPL activity was measured as the amount of free fatty acids released for each reaction as measured by relative light units after addition of colorimetric reagent to reaction incubations. Each reaction was performed in triplicate. **D.** IC_{50} concentration of apoC-III for WT vs. A43T from the activity curves in C. Each bar represents triplicate reactions. All data was replicated twice by two independent repeat experiments. For all data presented here, 1 μM apoC-III = 0.088 mg/dL apoC-III. All measurements show mean ± S.E.M. where appropriate, and data and spread show technical replicate values. **P<0.01, ***P<0.001, Student's unpaired two-tailed T-test.

Supplementary Figure 13

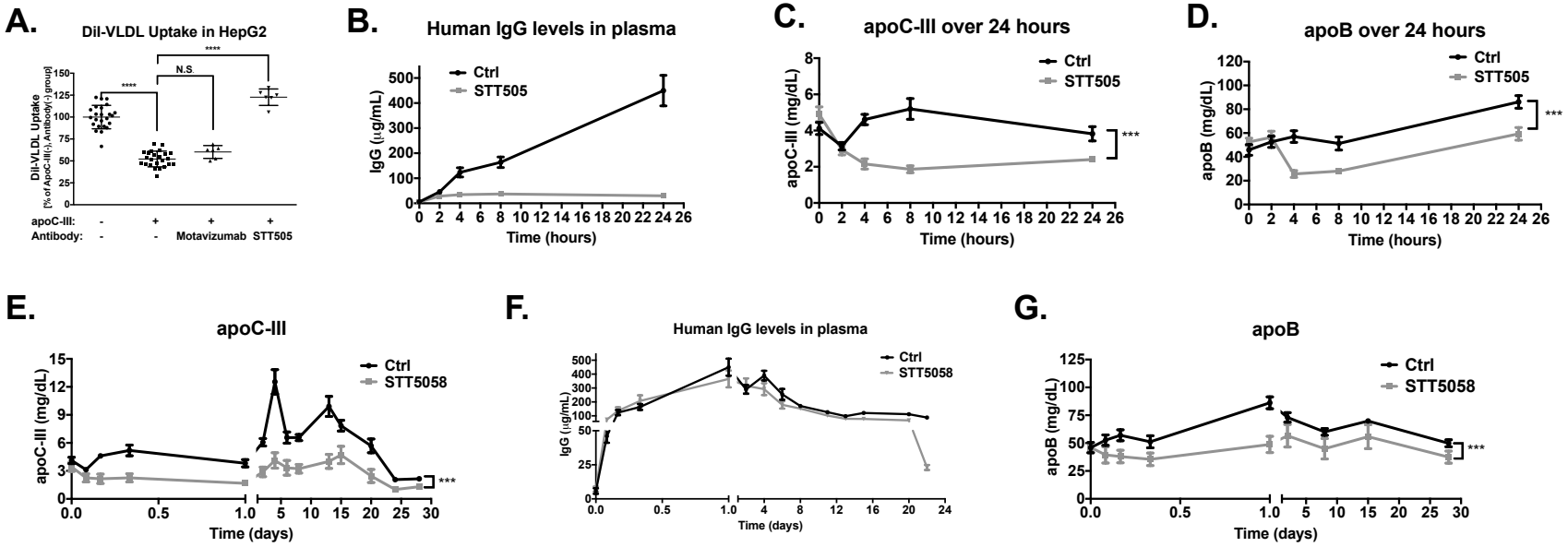

Supplementary Figure 13: Testing of STT505 and STT5058 monoclonal antibodies in vitro and in vivo. A. Uptake of DiI-labeled human VLDL by HepG2 cells. ApoC-III (3 µM or 0.264 mg/dl concentration), test antibody (0.072 mg/dl), media and 0.0125% BSA were combined to a final volume of 50 µl for each test reaction. These mixtures were incubated for 15 minutes at 37°C, and then were mixed with 30 µg/µl apoC-III-depleted DiI VLDL for an additional 20 minutes at 37°C. These final mixtures were then added to HepG2 cells at confluency in 96-well poly-D-lysine plates and reaction mixtures with HepG2 cells were incubated for 3.5 hours at 37°C. Following this incubation, cells were washed with 100 µl of 1% Intralipid diluted in MEM and then washed with 200 µl of PBS and then 100 µl isopropanol with gentle shaking. Isopropanol extracts were used to measure fluorescence (ex = 520 nm;

em = 580 nm), and this was compared to the fluorescence from a DiI VLDL standard curve to determine the amount of DiI VLDL per volume in the cell reactions. The remaining reactions on the cell plates were lysed with 0.1 N NaOH + 0.1% SDS and protein measured by BCA assay. The quantity of VLDL internalized was calculated as the DiI VLDL/protein ratio. For this experiment, motavizumab was used as a control antibody and compared to STT505 prior to uptake assays for indicated groups. N=3 technical replicates per group. Data was replicated by a repeat experiment once. **B.** Plasma human IgG levels following treatment of *APOC3* WT AAV-expressing WT mice with control or STT505 antibody at the zero time point for up to 24 hours as measured by autoanalyzer. **C.** Plasma apoC-III levels in mice from B over 24 hours as measured by autoanalyzer (correlating with the values normalized to the control apoC-III levels shown in Figure 4B). D. Plasma apoB levels in mice from B over 24 hours as measured by autoanalyzer (correlating with the values normalized to the control apoC-III levels shown in Figure 4D). For B-D, all data show experiments with N=8 mice treated with STT505 antibody and N=10 control-treated mice. Each experiment was replicated once by an independent repeat experiment. **E.** Plasma apoC-III levels following treatment of *APOC3* WT AAV-expressing WT mice with control or STT5058 antibody (25 mg/kg subcutaneously dosed) for 28 days as measured by autoanalyzer (correlating with the values normalized to the control apoC-III levels shown in Figure 4J). **F.** Plasma human IgG levels in mice from E as measured by autoanalyzer. **G.** Plasma apoB levels in mice from E as measured by autoanalyzer (correlating with the values normalized to the control apoB levels shown in Figure 4K). For E-G, all data show experiments with N=7 mice treated with STT5058 antibody and N=7 isotype control-treated mice. Each experiment was replicated once by an independent repeat experiment. All measurements show mean ± S.E.M. where appropriate. For A, ****P<0.0001, Student's unpaired T-test of comparison of the indicated groups. For all other panels, ***P<0.001, 2-way ANOVA.

Supplemental Tables and Legends

Supplementary Table 1: Predicted Impact of *APOC3* LoF Variants on mRNA processing and splicing							
R19X (g.116701353C>T; rs76353203)							
Genomic Coordinates	**Position relative to natural site**	**Initial(Ri)**	**Final(Ri)**	**Δ Ri**	**Fold change**	**% Binding (Final/Initial)**	**Predicted Change**
hnRNP H binding prediction							
116701372	19	0.9	0.9	0	1	100	No change
116701378	25	4.4	4.4	0	1	100	No change
116701379	26	4.2	4.2	0	1	100	No change
116701386	33	4.8	4.8	0	1	100	No change
hnRNP A1 binding prediction							
116701318	-35	1.5	1.5	0	1	100	No change
116701321	-32	1.5	1.5	0	1	100	No change
116701332	-21	0.1	0.1	0	1	100	No change
116701362	9	2.4	2.4	0	1	100	No change
116701371	18	2.2	2.2	0	1	100	No change
116701376	23	4.7	4.7	0	1	100	No change
116701377	24	0.3	0.3	0	1	100	No change
116701383	30	4.9	4.9	0	1	100	No change
116701388	35	0.5	0.5	0	1	100	No change
116701398	45	4.5	4.5	0	1	100	No change
116701399	46	1.2	1.2	0	1	100	No change
116701352	***-1***	***-4.5***	***4.7***	***9.2***	***26.1***	***2610.9***	***Increased***
Genome-wide splice donor prediction							
116701311	-42	0.3	0.3	0	1	100	No change
116701354	***1***	***2.5***	***3.8***	***1.3***	***2.5***	***249.1***	***Increased***
116701365	12	2.5	2.5	0	1	100	No change
116701387	34	1.3	1.3	0	1	100	No change
Gene-specific splice-donor prediction							

116701311	-42	1.8	1.8	0	1	100	No change
116701354	***1***	***5.2***	***6***	***0.7***	***1.7***	***165.8***	***Increased***
116701365	12	4.2	4.2	0	1	100	No change
116701387	34	3	3	0	1	100	No change
Splice branch-point prediction							
116701396	43	0.4	0.4	0	1	100	No change
Genome-wide splice-acceptor prediction							
116701334	-19	0	0	0	1	100	No change
Gene-specific splice-acceptor prediction							
116701334	-19	3.3	3.3	0	1	100	No change
116701335	-18	0	0	0	1	100	No change
116701343	-10	1.2	1.2	0	1	100	No change
116701358	***5***	***1.3***	***1.5***	***0.2***	***1.1***	***114***	***Increased***
116701357	***4***	***-0.5***	***0.1***	***0.6***	***1.1***	***107.8***	***Increased***
IVS2+1 G>A (g.116701354 G>A; rs138326449)							
Genomic Coordinates	**Position relative to natural site**	**Initial(Ri)**	**Final(Ri)**	**Δ Ri**	**Fold change**	**% Binding (Final/Initial)**	**Predicted Change**
hnRNP H binding prediction							
116701372	18	0.9	0.9	0	1	100	No change
116701378	24	4.4	4.4	0	1	100	No change
116701379	25	4.2	4.2	0	1	100	No change
116701386	32	4.8	4.8	0	1	100	No change
hnRNP A1 binding prediction							
116701318	-36	1.5	1.5	0	1	100	No change
116701321	-33	1.5	1.5	0	1	100	No change
116701332	-22	0.1	0.1	0	1	100	No change
116701362	8	2.4	2.4	0	1	100	No change
116701371	17	2.2	2.2	0	1	100	No change
116701376	22	4.7	4.7	0	1	100	No change
116701377	23	0.3	0.3	0	1	100	No change

116701383	29	4.9	4.9	0	1	100	No change
116701388	34	0.5	0.5	0	1	100	No change
116701398	44	4.5	4.5	0	1	100	No change
116701399	45	1.2	1.2	0	1	100	No change
Genome-wide splice donor prediction							
116701311	-43	0.3	0.3	0	1	100	No change
116701365	11	2.5	2.5	0	1	100	No change
116701387	33	1.3	1.3	0	1	100	No change
116701354	***0***	***2.5***	***-16.1***	***-18.6***	***-5.8***	***NA***	***Decreased***
Gene-specific splice-donor prediction							
116701311	-43	1.8	1.8	0	1	100	No change
116701365	11	4.2	4.2	0	1	100	No change
116701387	33	3	3	0	1	100	No change
116701354	0	5.2	-7.6	-12.8	-38	NA	Decreased
Splice branch-point prediction							
116701396	42	0.4	0.4	0	1	100	No change
Genome-wide splice-acceptor prediction							
116701334	-20	0	0	0	1	100	No change
Gene-specific splice-acceptor prediction							
116701334	-20	3.3	3.3	0	1	100	No change
116701335	-19	0	0	0	1	100	No change
116701343	-11	1.2	1.2	0	1	100	No change
116701358	***4***	***1.3***	***1.6***	***0.3***	***1.2***	***123.3***	***Increased***
A43T (g.116701560 G>A; rs147210663)							
Genomic Coordinates	**Position relative to natural site**	**Initial(Ri)**	**Final(Ri)**	**Δ Ri**	**Fold change**	**% Binding (Final/Initial)**	**Predicted Change**
hnRNP H binding prediction							
116701531	-29	1	1	0	1	100	No change
116701580	20	1.2	1.2	0	1	100	No change
hnRNP A1 binding prediction							

116701530	-30	4.9	4.9	0	1	100	No change
116701539	-21	4.6	4.6	0	1	100	No change
116701563	3	4.6	4.6	0	1	100	No change
116701572	12	2.4	2.4	0	1	100	No change
116701584	24	5.2	5.2	0	1	100	No change
116701585	25	0.1	0.1	0	1	100	No change
116701593	33	3	3	0	1	100	No change
Genome-wide splice donor prediction							
116701596	36	2.2	2.2	0	1	100	No change
Gene-specific splice-donor prediction							
116701596	36	4.2	4.2	0	1	100	No change
Splice branch-point prediction							
116701521	-39	1.3	1.3	0	1	100	No change
116701555	-5	0.9	0.9	0	1	100	No change
116701564	4	0.4	0.9	0.5	1.4	140	Increased
116701575	15	1.1	1.1	0	1	100	No change
Genome-wide splice-acceptor prediction							
116701532	-28	6	6	0	1	100	No change
Gene-specific splice-acceptor prediction							
116701532	-28	9.7	9.7	0	1	100	No change
116701607	47	0.3	0.3	0	1	100	No change
IVS3+1 G>T (g.116701613G>T; rs140621530)							
Genomic Coordinates	**Position relative to natural site**	**Initial(Ri)**	**Final(Ri)**	**Δ Ri**	**Fold change**	**% Binding (Final/Initial)**	**Predicted Change**
hnRNP H binding prediction							
116701580	-33	1.2	1.2	0	1	100	No change
116701606	***-7***	***3***	***-1.9***	***-4.9***	***-8.2***	***NA***	***Decreased***
hnRNP A1 binding prediction							
116701563	-50	4.6	4.6	0	1	100	No change
116701572	-41	2.4	2.4	0	1	100	No change

116701584	-29	5.2	5.2	0	1	100	No change
116701585	-28	0.1	0.1	0	1	100	No change
116701593	-20	3	3	0	1	100	No change
116701610	***-3***	***3.9***	***3.1***	***-0.9***	***-1.8***	***54.8***	***Decreased***
Genome-wide splice donor prediction							
116701596	-17	2.2	2.2	0	1	100	No change
116701613	***0***	***3***	***-15.6***	***-18.6***	***-8.1***	***NA***	***Decreased***
Gene-specific splice-donor prediction							
116701596	-17	4.2	4.2	0	1	100	No change
116701613	***0***	***4.5***	***-3.3***	***-7.8***	***-22.9***	***NA***	***Decreased***
Splice branch-point prediction							
116701564	-49	0.4	0.4	0	1	100	No change
116701575	-38	1.1	1.1	0	1	100	No change
116701637	24	1	1	0	1	100	No change
Genome-wide splice-acceptor prediction							
116701650	37	4.3	4.3	0	1	100	No change
Gene-specific splice-acceptor prediction							
116701607	-6	0.3	0.3	0	1	100	No change
116701646	33	1.7	1.7	0	1	100	No change
116701650	37	9.4	9.4	0	1	100	No change
116701653	40	0.7	0.7	0	1	100	No change
116701638	***25***	***-0.3***	***0.6***	***0.9***	***1.5***	***146.9***	***Increased***

Supplementary Table 1: Predicted impact of *APOC3* LoF variants on APOC3 mRNA splicing. Each of the four *APOC3* LoF variants were assessed for impact on interaction with mRNA processing machinery and on the relative energetic changes to splice-donor and splice-acceptor site usage using the Automated Splice Site and Exon Definition Analyses information theory based prediction tool (http://splice.uwo.ca/). Genomic Coordinates indicate genomic position

on chromosome 11 for which a particular prediction is made. Position relative to the natural site indicates the position on the (+) strand of the variant assessed relative to the Genomic Coordinates. Initial and Final Ri indicate the information content of the base in the WT or variant form, respectively, and ΔRi indicates the difference between Final Ri and Initial Ri. Fold change indicates the difference in binding affinity for a site in the variant vs. WT form based on the ΔRI. % Binding indicates the percentage increase or decrease in binding propensity for a given binding factor. Predicted change indicates the overall predicted effect for the given measure based on the ΔRi and predicted fold change for a given position.

Nature Medicine: doi:10.1038/nm.4390

Supplementary Table 2: List of mouse standard samples for multiple reaction monitoring assays				
Sample ID	**Total apoC-III concentration (µg/µl)**	**Final WT concentration (µg/µl)**	**Final A43T concentration (µg/µl)**	**Molar ratio of concentrations**
Std01	0.134	0.134	0	0
Std02	0.092	0.09	0.002	0.03
Std03	0.03	0.02	0.01	0.5
Std04	0.026	0.015	0.011	0.75
Std05	0.023	0.012	0.012	1

Supplementary Table 2: List of mouse standard samples for multiple reaction monitoring assays

Plasma from mice expressing exclusively WT or A43T apoC-III through AAV-mediated expression was quantified for apoC-III concentration and mixed at the indicated molar ratios for standardization of the relative mutant:WT protein ratios identified from multiple reaction monitoring.

Supplementary Table 3: List of selected apoC-III peptides and transitions for multiple reaction monitoring assays					
Protein	**Peptide name**	**Peptide sequence**	**CE**	**Light SRM (m/z)**	**Heavy SRM (m/Z)**
apoC-III	Thr43 Oxi	DASLLSFM(oxi)QGYM(oxi)KH ATKTTK	24.7	573.3 → 702.0 635.3 597.6 568.1	575.0 →704.4 637.6 597.6 568.6
apoC-III	Ala43 Oxi	DASLLSFM(oxi)QGYM(oxi)KH ATKTAK	24.5	565.8 → 692.0 625.3 587.6 558.6	567.5 → 694.3 627.7 587.6 558.6
apoC-III	DGF	DGFSSLK	14.5	377.2 → 581.3 434.3 347.2	
apoC-III	DYW	DYWSTVK	17.1	449.7 → 620.3 434.3 347.3	
SERPIN B14	DIL	DILNQITKPN	21.8	578.3 → 459.3 358.2 230.1	

Supplementary Table 3: List of selected ApoC-III peptides and transitions for multiple reaction monitoring assays

Peptides spanning the 23rd residue of apoC-III were analyzed for fragmentation and transition ion mass to charge (m/Z) ratios were monitored in the multiple reaction monitoring assays. Heavy amino acids are underlined (^{13}C, ^{15}N). CE, collision energy.

Supplementary Table 4: Plasma Lipids in Murine Models of WT vs. A43T *APOC3* Expression																		
Measurement:	**Total Cholesterol (mg/dL)**			**HDL-C (mg/dL)**			**NonHDL-C (mg/dL)**			**TG (mg/dL)**			**Human apoC-III (mg/dL)**			**Human apoB (mg/dL)**		
Group:	Null	WT	A43T	Null	WT	A43T	Null	WT	A43T	Null	WT	A43T	Null	WT	A43T	Null	WT	A43T
C57BL/6 WT	95.8 (5.4)	97.0 (3.4)	94.3 (8.4)	76.2 (5.7)	73.8 (4.3)	73.5 (8.3)	19.7 (1.0)	23.2 (2.9)	20.9 (1.3)	**46.0 (10.2)**	**104.8 (21.0)**	**58.2 (15.6) ****	**0.0 (0.0)**	**14.8 (3.0)**	**6.0 (1.4) **** / ††††**			
Apoc3 KO	86.4 (12.3)	101.0 (9.7)	90.6 (4.4)	65.3 (11.6)	74.9 (7.2)	70.7 (6.4)	**21.1 (2.0)**	**26.1 (3.5)**	**19.9 (2.1) ****	**33.0 (2.4)**	**76.4 (15.5)**	**43.6 (7.3) ** / †**	**0.0 (0.0)**	**14.2 (1.2)**	**3.8 (3.2) *** / †**			
LahB WT	157.7 (11.4)	169.8 (8.6)	166.3 (14.8)	83.8 (7.0)	76.7 (6.1)	75.2 (6.1)	**73.9 (5.3)**	**93.1 (5.6)**	**91.1 (9.0) †**	**165.5 (10.1)**	**260.6 (33.3)**	**190.2 (22.2) ** / †**	**0.0 (0.0)**	**13.7 (2.6)**	**6.4 (1.9) *** / ††††**			
LahB Het	291.3 (26.1)	268.5 (28.3)	281.2 (7.4)	108.7 (7.3)	113.4 (10.0)	114.0 (3.8)	182.6 (18.9)	155.1 (19.4)	167.2 (7.9)	**268.3 (29.1)**	**335.8 (73.0)**	**257.4 (5.5) ***	**0.0 (0.0)**	**24.0 (13.4)**	**5.4 (4.5) * / †**	171.4 (12.4)	147.1 (19.0)	157.9 (7.4)
C57BL/6 WT + CETP	69.0 (20.2)	58.7 (4.9)	58.7 (2.1)	**43.7 (19.4)**	**21.9 (2.9)**	**32.9 (2.4) ******	**25.3 (5.7)**	**36.7 (2.5)**	**25.8 (1.2) ******	**61.3 (10.2)**	**252.0 (18.7)**	**90.7 (14.6) **** / ††**	**0.0 (0.0)**	**16.4 (1.8)**	**4.5 (1.0) **** / ††††**			
Apoc3 KO + CETP	70.8 (15.5)	63.8 (5.9)	61.6 (3.0)	**43.4 (14.3)**	**26.3 (4.3)**	**33.6 (2.9) ***	**27.5 (5.3)**	**37.5 (6.5)**	**27.8 (2.5) ****	**42.3 (9.2)**	**192.4 (35.8)**	**55.0 (14.2) ******	**0.0 (0.0)**	**16.7 (2.2)**	**2.4 (1.6) **** / †††**			
LahB KO + CETP	376.0 (139.4)	575.6 (90.2)	457.6 (133.6)	119.7 (38.3)	139.4 (8.6)	140.1 (12.2)	**256.3 (103.5)**	**436.2 (92.2)**	**317.5 (127.6) ***	**124.2 (60.2)**	**242.0 (74.0)**	**144.4 (64.2) ***	**0.0 (0.0)**	**16.5 (1.3)**	**3.9 (3.3) **** / †**	**121.0 (85.9)**	**210.2 (59.2)**	**146.8 (85.8) ***

Supplementary Table 4: Plasma lipids in murine models of WT vs. A43T *APOC3* expression. Measurements [mean values(S.D.)] are given for each group of mice expressing Null, WT *APOC3*, or A43T *APOC3* AAVs by intraperitoneal administration at a dose of $3x10^{11}$ genome copies (GC)/mouse. Measurements show data from plasma drawn after four hours of fasting at four weeks after AAV administration. Each experiment utilized N=6 male mice per group at approximately 10-12 weeks of age. LahB WT mice are *Apobec1* KO; human *APOB* transgenic; *Ldlr* WT mice. LahB Het mice are *Apobec1* KO; human *APOB* transgenic; *Ldlr* heterozygous mice. LahB KO mice are *Apobec1* KO; human *APOB* transgenic; *Ldlr* KO mice. Groups with "+CETP" were co-transduced with $3x10^{10}$ GC/mouse of human *CETP* AAV vector along with the indicated Null or *APOC3* AAV vectors. Bold sets of data indicate significant results (P<0.05) by two-way

ANOVA. *P<0.05, **P<0.01, ***P<0.001, ****P<0.0001, comparison of WT and A43T groups by Tukey's post-test after two-way ANOVA. † P<0.05, †† P<0.01, ††† P<0.001, †††† P<0.0001, comparison of Null and A43T groups by Tukey's post-test after two-way ANOVA.